TRANSLATIONAL AND CLINICAL RESEARCH

Reversing Bone Loss by Directing Mesenchymal Stem Cells to Bone

WEI YAO,[a] MIN GUAN,[a] JUNJING JIA,[a] WEIWEI DAI,[a] YU-AN E. LAY,[a] SARAH AMUGONGO,[a] RUIWU LIU,[b] DAVID OLIVOS,[b] MARY SAUNDERS,[b,c] KIT S. LAM,[a,b] JAN NOLTA,[c] DIANA OLVERA,[d] ROBERT O. RITCHIE,[d] NANCY E. LANE[a]

[a]Department of Internal Medicine, University of California at Davis Medical Center, Sacramento, California, USA; [b]Department of Biochemistry and Molecular Medicine, University of California at Davis Medical Center, Sacramento, California, USA; [c]Department of Internal Medicine, Stem Cell Program and Institute for Regenerative Cures, University of California at Davis Medical Center, Sacramento, California, USA; [d]Department of Materials Science and Engineering, University of California at Berkeley, Berkeley, California, USA

ABSTRACT

Bone regeneration by systemic transplantation of mesenchymal stem cells (MSCs) is problematic due to the inability to control the MSCs' commitment, growth, and differentiation into functional osteoblasts on the bone surface. Our research group has developed a method to direct the MSCs to the bone surface by conjugating a synthetic peptidomimetic ligand (LLP2A) that has high affinity for activated α4β1 integrin on the MSC surface, with a bisphosphonates (alendronate) that has high affinity for bone (LLP2A-Ale), to direct the transplanted MSCs to bone. Our in vitro experiments demonstrated that mobilization of LLP2A-Ale to hydroxyapatite accelerated MSC migration that was associated with an increase in the phosphorylation of Akt kinase and osteoblastogenesis. LLP2A-Ale increased the homing of the transplanted MSCs to bone as well as the osteoblast surface, significantly increased the rate of bone formation and restored both trabecular and cortical bone loss induced by estrogen deficiency or advanced age in mice. These results support LLP2A-Ale as a novel therapeutic option to direct the transplanted MSCs to bone for the treatment of established bone loss related to hormone deficiency and aging. STEM CELLS 2013;31:2003-2014

Disclosure of potential conflicts of interest is found at the end of this article.

INTRODUCTION

The aging segment of the population is rapidly expanding, and with it osteoporosis has become a significant health concern. The current treatment of osteoporosis is focused on agents, such as the bisphosphonates, selective estrogen receptor modulators, calcitonin, or receptor activator of nuclear factor kappa B ligand inhibitors, which reduce bone loss by decreasing osteoclastic bone resorption and thereby preventing further breakdown of bone. An important limitation of this class of drugs is that it does not restore the lost bone structure. The only therapeutic option that stimulates bone formation and is approved by Food and Drug Administration is teriparatide (recombinant human parathyroid hormone 1-34; rhPTH 1-34), an anabolic agent that is limited to 2 years of use and is only effective in about 60% of treated individuals [1]. One other bone anabolic agent, a humanized monoclonal antibody against sclerostin [2], a protein of which the majority of it is secreted by osteocytes and inhibits bone formation, is currently in a Phase III clinical trial to determine its efficacy and safety in postmenopausal women with osteoporosis.

Mesenchymal stem cells (MSCs) are multipotent cells present in bone marrow that have the potential to differentiate into osteoblasts and form bone [3]. Aging is associated with a reduction in marrow MSC numbers and a deficiency in the supportive mechanisms that are required for MSCs to augment bone formation [4,5]. The decrease in the resident MSC population with advanced age may be the most important factor responsible for reduced bone formation and the subsequent increase in bone fragility [6]. Therapeutic modalities that target bone formation by either increasing the number of and/or activity of osteoblasts may be a more attractive approach to enhance bone formation and promote bone regeneration. Bone regeneration through induction of MSCs will promote osteogenesis and provide a rational therapeutic strategy for preventing age-related osteoporosis.

Both autologous and allogeneic stem cells have been successfully infused into animals and humans for the treatment of degenerative heart, neuronal diseases, and for nerve or heart injury repairs [7–10]. However, systemic

transplantation of MSCs in vivo have failed to promote an osteogenic response in bone due to the inability of MSCs to home to the bone surface unless they were genetically modified [11–13] or after certain injuries [14,15]. This has become a major obstacle for MSC transplantation [16,17]. Even if the transplanted MSCs make it to "bone," they are usually observed engrafting in the upper metaphysis, epiphysis, or within the sinusoids of bone marrow or the Haversian canals [15,17,18]. The transplanted MSCs are removed from bone marrow within 4–8 weeks, and there is no evidence of long-term engraftment [15,17,18]. To overcome this obstacle in using MSCs for bone regeneration, we synthetized a peptidomimetic ligand LLP2A that had both high affinity and specificity for the integrin $\alpha4\beta1$ (IC50 = 2 pM) [19], which is highly expressed on the MSC surface. We conjugated this ligand, LLP2A, to alendronate, a bisphosphonate with high affinity for bone. The resulting hybrid compound, LLP2A-Ale, targets both bone and MSCs, with alendronate functioning as the bone-seeking component to direct LLP2A to bone, and LLP2A directs MSCs to the surface of bone [20]. In vitro, LLP2A-Ale increased MSC migration, the commitment of MSCs to osteoblast differentiation, osteoblast maturation and function as reflected by increased expression of Runx2 and osteocalcin (OC) and increased calcified matrix deposition. Furthermore, LLP2A-Ale did not affect either chondrogenic or adipogenic potential of the MSCs. Our proof-of-concept studies in animals indicated that LLP2A-Ale directs MSCs, naturally present or transplanted, toward bone to enhance bone formation. In untreated mice, infused human MSCs accumulated in lung, liver, and spleen while MSCs in the LLP2A-Ale treated animals were visually imaged only at the bone surface and were found embedded in bone matrix as osteocytes or adjacent to the bone surface as osteoblasts 21 days after the transplantation [20,21]. In this report, we performed additional experiments demonstrating LLP2A-Ale's ability to direct MSC migration and osteoblast differentiation is highly dependent on bone microenvironments, that is, extracellular matrix (ECM) proteins and hydroxyapatite. More importantly, we evaluated the treatment efficacy of LLP2A-Ale in clinical relevant animal models of bone loss, including bone loss induced by estrogen deficiency and aging. We found that LLP2A-Ale + systemic MSC transplantation greatly increased bone formation and bone strength in both the trabecular and cortical bone in mice with established osteopenia associated with estrogen deficiency or advanced aging. We demonstrated that LLP2A-Ale overcomes the challenges of MSCs bone homing and that it also influences MSC's lineage commitment, growth, and differentiation into functional osteoblasts on the bone surface, making LLP2A-Ale an efficacious therapy for restoring bone loss related to age and hormone deficiency.

MATERIALS AND METHODS

Animal Experimental Groups

OVX Study. Groups of C57BL/6 mice were ovariectomized (OVX) at 2 months of age. Two weeks after OVX, the mice were treated with phosphate-buffered saline (PBS), LLP2A, MSC (5×10^5), LLP2A-Ale (0.9 nmol/mouse, IV at weeks 2, 6, and 10; total estimated alendronate dose was 2.2 μg/mouse), MSC + LLP2A (LLP2A-Ale and MSCs were mixed together then given by IV at weeks 2, 6, and 12), or human PTH (1-34) (30 μk/kg, threee time per week; Bachem, Inc., Torrance, CA). Mice were killed at week 14 (n = 8–14 per group).

Aging Studies. Female mice of 24 week or 24 months old were treated with either PBS, LLP2A, MSC (5×10^5), LLP2A-Ale (0.9 nmol/mouse, IV at baseline and week 6; total estimated alendronate dose was 1.5 μg/mouse), MSC + LLP2A (LLP2A-Ale and MSCs were mixed together then treated by IV at baseline and week 6), or human PTH (1-34) (30μk/kg, 5 itmes per week). Mice were killed at week 12 (n = 8–14 per group).

All animals were maintained in the Animal Facility of the UC Davis Medical Center. The experimental protocols were approved by the Institutional Animal Care and Use Committee of UC Davis, Davis, CA.

In Vitro Migration and Osteogenesis Assays

Cell migration assays were performed using Transwell migration chambers coated with bovine serum albumin (BSA) or with 10 μg/mL collagen types I and IV (Col I and Col IV), fibronectin (FN), or laminin (LAM). The coated filters were rinsed with PBS and placed into the lower chamber containing serum-free medium supplemented with 45 nM LLP2A-Ale. Bone marrow-derived MSCs (Texas A&M Health Science Center under a material transfer agreement between UC Davis and the Institute for Regenerative Medicine in Texas A&M HSC COM (Temple, TX)) were added to the upper compartment of the Transwell chamber at 50,000 per well and allowed to migrate to the underside of the top chamber for 8 hours in serum-free media. Half of the bottom wells were precoated with 10% hydroxyapatite. The cells that did not migrate on the upper membrane were removed and the cells that migrated attached to the bottom surface of the membrane and were fixed with 10% formaldehyde for 1 hour, and the cells remaining on the top of the polycarbonate membrane were removed. The cells that had migrated through the pores to the lower surface were stained with crystal violet. Subsequently, stained cells were eluted from membranes and absorbance measure at 590 nm [20]. On days 14 of the culture, the colony forming units (CFU) were stained by crystal violet (CFU-F) followed by with alkaline phosphatase (ALP) staining for ALP+ colonies (CFU-Ob) (Sigma-Aldrich, St. Loius, MO http://www.sigmaaldrich.com). Subsequently, stained cells were eluted from membranes and absorbance measure at 590 nm (crystal violet) or 410 nm (ALP).

Receptor Tyrosine Kinases (RTK)-Phospho Array and Western Blotting

Bone marrow-derived MSCs were cultured to nearly 70%–80% confluent in regular dishes or in dishes coated with hydroxyapatite as described above, they were then incubated with PBS or LLP2A-Ale (45 nM) for 30 minutes, 2 hours, or 4 hours. After the incubations, cells were trypsinized, washed and lysed. Protein concentration was measured using the Bio-Rad protein assay kit (Richmond, CA). The PathScan RTK Signaling Antibody Array Kit (Chemiluminescent Readout) was used according to the manufacturer's instructions (Cell Signaling, Beverly, MA http://www.cellsignal.com). This kit is a slide-based antibody array founded upon the sandwich immunoassay principle. The array kit allows for the simultaneous detection of 28 receptor tyrosine kinases and 11 important signaling nodes, when phosphorylated at tyrosine or other residues. Target-specific capture antibodies, biotinylated protein (positive control) and nonspecific immunoglobulin G (IgG; negative control) have been spotted in duplicate onto nitrocellulose-coated glass slides. Western blot analyses were performed to measure total and phosphorylated Akt and S6-Ribosomal (rpS6) kinase proteins. Cells were lysed in cold buffer containing 20 mM Tris (pH 7.5), 150 mM NaCl, 1 mM EDTA, 1 mM EGTA, 1% Triton X-100, 2.5 mM sodium pyrophosphate, 1 mM β-Glycerophosphate, 15 mmol/l NaF, 1 μg/mL Leupeptin, 1 mM PMSF, and centrifuged at 12,000 rpm for 10 minutes. The protein extracts (10 μg/lane) were subjected to electrophoresis on 4-10% SDS-polyacrylamide gel electrophoreses gel and transferred to a PVDF membrane, which was stained by Naphthol Blue-Black

to confirm equal protein loading. The membranes were blocked in BSA for 1 hour and then incubated with the following primary antibodies: Akt, phosphor-Akt (Ser473), rpS6, phosphor- rpS6 antibodies (Cell Signaling Technology, Beverly, MA). Membranes were then incubated with horseradish peroxidase-conjugated goat anti-rabbit or anti-mouse IgG secondary antibody and detection was done using supersignal west pico stable peroxide solution (Pierce, Rockford, IL http://www.piercenet.com). Films were scanned and band densities were analyzed using a BIO-RAD ChemiDoc MP Imaging system (Bio-Rad Life Science Research, Hercules, CA http://www.bio-rad.com).

Immunohistochemistry

Bone samples were fixed in 4% paraformaldehyde, decalcified in 10% ethylenediaminetetraacetic acid (EDTA) for 10 days, and embedded in paraffin. Sections of 4-μm were obtained and incubated in 3% hydrogen peroxide in water to block endogenous peroxidases. The slides were incubated with 1% normal goat serum in Tween 20 in PBS, before incubation with the green fluorescent protein (GFP) or osteocalcin antibodies (Cell Signaling Technology, Beverly, MA). The sections were incubated with the Alexa Fluor 488 conjugated goat anti-rabbit or Alexa Fluor 594 conjugated goat anti-mouse secondary antibodies for detection.

Bone Histomorphometry

Mice received subcutaneous injections of alizarin red (20 mg/kg) at baseline and calcein (10 mg/kg) 7 and 2 days before killing. The fifth lumbar vertebral bodies, the right distal femurs and mid-femurs were dehydrated and embedded undecalcified in methyl methacrylate. Sections were either stained in tetrachrome or left unstained sections were used for assessing fluorochrome labeling and dynamic changes in bone. Bone histomorphometry was performed using a semi-automatic image analysis system (Bioquant Image Analysis Corp., Nashville, TN http://www.bioquant.com) [22–25].

Micro-CT

The right distal femur from each of the animals was scanned using micro-CT with an isotropic resolution of 10 μm in all three spatial dimensions. Mineralized bone was separated from the bone marrow with a matching cube three-dimensional segmentation algorithm. A normalized index, trabecular bone volume/total volume (BV/TV), was used to compare samples of varying size. Trabecular thickness (Tb.Th), trabecular separation (Tb.Sp), and trabecular number (Tb.N) were also calculated [22,23].

Biomechanical Testing

For the vertebrae, the endplates of the lumbar vertebral body were polished using an 800-grit silicon carbide paper to create two parallel planar surfaces. Each lumbar vertebra was then loaded to failure under far-field compression along its long axis using an MTS 831 electro-servo-hydraulic testing system (MTS Systems Corp., Eden Prairie, MN) at a displacement rate of 0.01 mm/second with 90) N load cell; sample loads and displacements were continuously recorded throughout each test. To analyze the biomechanical properties of the tibiae, the ends of each tibia were removed. The tibia samples were subjected to three-point bending tests, with the bone loaded using an EnduraTEC Electro Force 3,200 testing system (Bose Corp., Eden Prairie, MN http://worldwide.bose.com) such that the posterior surface was in tension and the anterior surface was in compression; the major loading span was 14.5 mm. Each tibia was loaded to failure in 37°C HBSS at a displacement rate of 0.01 mm/second while its corresponding load and displacement were measured using a calibrated 225 N load cell. Values for the maximum load, maximum stress (bone strength) for compression and maximum load, and ultimate strength of bending tests were then determined [22,23,26].

Statistical Analyses

The group means and SDs were calculated for all outcome variables. Nonparametric Kruskal-Wallis test and Tamhane Post Hoc were used to determine the differences between the groups. Differences were considered significant at $p < .05$ (IBM SPSS Statistics 20; SPSS Inc., Chicago, IL).

RESULTS

LLP2A-Ale-Induced MSC Migration Was Extracellular Matrix Specific and Was Associated with Increased Akt Tyrosine Kinases Phosphorylation

As the ECM made by bone marrow cells plays an important role in the maintenance of MSC function, migration and osteoblast differentiation [27–31], and LLP2A-Ale increased MSC migration in vitro [20], we first evaluated if different compositions of the marrow ECM would affect LLP2A-Ale induced MSC migration. MSC migration was examined using a 24-well transwell system where the inserts were procoated with 10 μg/ ml of FN, LAM, Col 1 or Col IV. MSCs were placed into the top inserts precoated with different ECMs at a concentration of 15×10^4/well. The cells were allowed to migrate in serum-free conditions with or without LLP2A-Ale, and with or without hydroxyapatite microparticle-coated bottom well for 8 hours. Hydroxyapatite is the main component of bone mineral and alendronate has very high affinity to the calcium component of the hydroxyapatite. In the absence of coated hydroxyapatite we observed an increase in MSC migration when the cells were plated on Col I (93% higher vs. control, $p < .05$), FN (19% higher than control), LAM (55% higher than control) (Fig. 1A). When the bottom well was coated with hydroxyapatite, most if not all of the LLP2A-Ale would have been immobilized, MSCs migration increased significantly, particularly when the transwell was coated with Col I (118% higher than control, $p < .05$) and Col IV (56% higher than control) (Fig. 1B). While LLP2A-Ale slightly increased MSC migration in transwell without the bottom well coated with the hydroxyapatite (Fig. 1C), MSC migration was increased by more than 300% ($p < .05$) when the bottom well was coated with hydroxyapatite (Fig. 1D). These results confirmed our previous finding that LLP2A-Ale increased MSC migration [20]. More importantly, LLP2A-Ale increased MSC migration toward hydroxyapatite, the main component of mineralized tissue and in the presence of Col I, a principal component of bone matrix protein and Col IV, a major structural component of basement membranes that also expresses α1.

As the migration capacity of bone marrow MSCs is under the control of a large numbers of receptor tyrosine kinases (RTKs) in response to growth factors or chemokines [32–34], we evaluated how LLP2A-Ale regulates RTK activation in MSCs and their migration with or without the presence of hydroxyapatite. We cultured mouse bone marrow-derived MSCs with or without hydroxyapatite and LLP2A-Ale for 30 minutes, 2 and 4 hours, then used a mouse slide-based antibody array to screen and simultaneously determine the relative quantification of 28 RKTs that are phosphorylated at tyrosine or other residues (Cell Signaling Technology Inc., Danvers, MA). MSCs cultured with LLP2A-Ale has higher immunoreactivity for Akt (Thr308 and Ser473) and S6 Ribosomal protein (rpS6), which started to increase at 30 minutes and reached its peak compared with the control group after 2 hours (Fig. 1E). When MSCs were plated onto hydroxyapatite that were in contact with LLP2A-Ale and hydroxyapatite, all the RTKs were
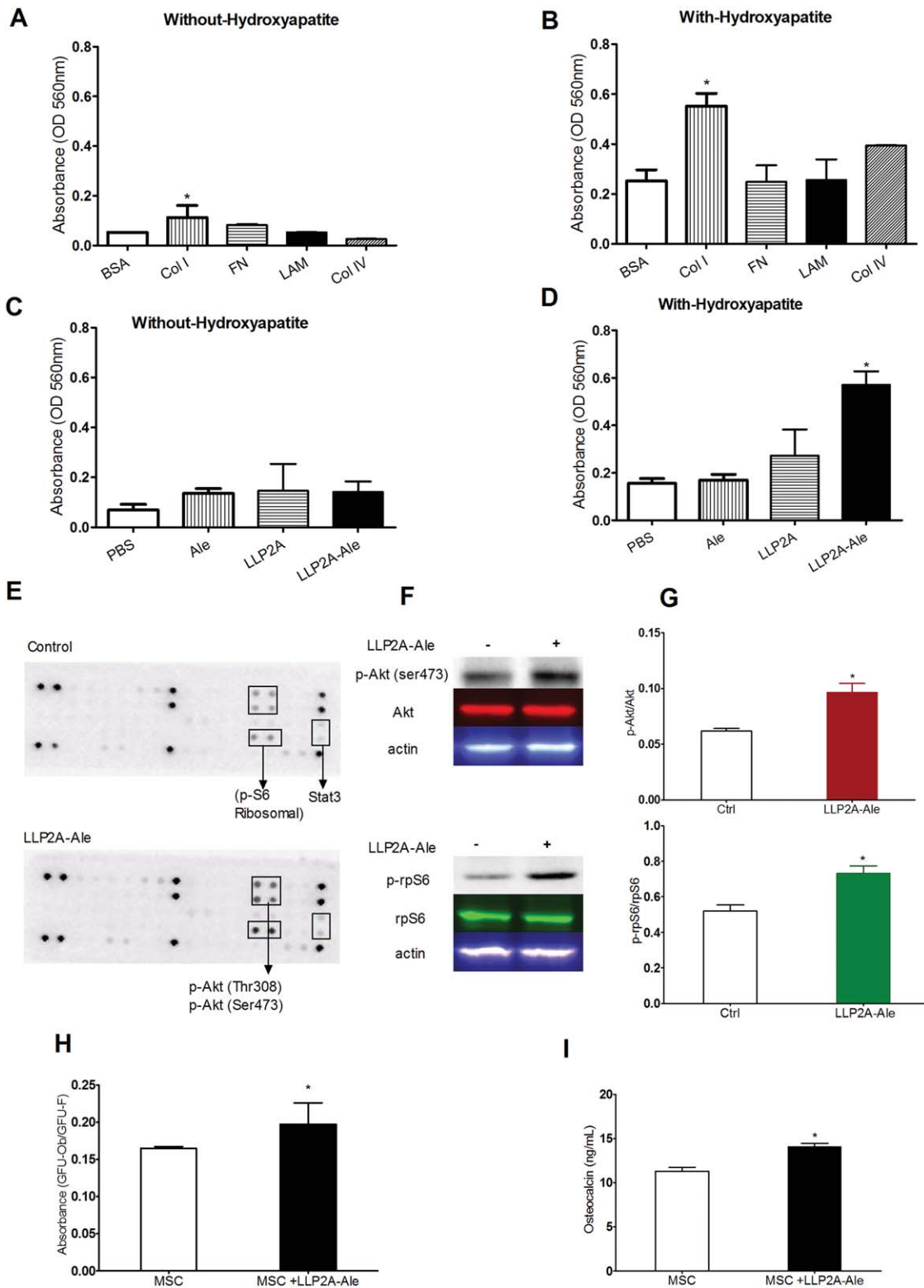
Figure 1. LLP2A-Ale induced mesenchymal stem cell (MSC) migration was matrix and mineral dependent. **(A):** Mouse bone marrow-derived MSCs were seeded in the upper chamber of transwell plates with inserts that were precoated with bovine serum albumin (BSA) or 10 μg/ml collagen type I (Col I), fibronectin (FN), laminin (LAM), or collagen type IV (Col IV) in serum-free conditions. The bottom wells were loaded with either media alone or containing 45 nM LLP2A-Ale. The cells that had migrated through the pores to the lower surface of the membrane were stained with crystal violet. Subsequently, stained cells were eluted from membranes and absorbance measure at 590 nm. **(B):** A similar set of experiments was performed as described in "**(A)**" except that the bottom wells were precoated with 10% hydroxyapatite. **(C):** A similar set of experiments was performed as described in "**(A)**" that the upper chamber of transwell plates with inserts were precoated with 10 μg/ml Col I in serum-free conditions. The bottom wells were loaded with either media alone or containing 45 nM Alendronate (Ale), LLP2A, or LLP2A-Ale. **(D):** Same experiments were performed as described in "**(C)**" except that the bottom wells were precoated with 10% hydroxyapatite. **(E):** Murine phosphorylated RTK arrays were used to examine Col I-induced RTK phosphorylation levels in MSC lysates without hydroxyapatite or with hydroxyapatite following LLP2A-Ale (45 nM) for 2 hours. **(F):** Western blotting analyses were performed for total Akt, rpS6, phosphorylated Akt, rpS6, and actin. **(G):** Quantitation for **(F)**. **(H):** MSCs were cultured with LLP2A-Ale for 10 days. Ratio of CFU-Ob/CFU-F was measured. **(I):** Osteocalcin levels were measured in for media in experiment described in "**(H)**". Experiments were performed in duplicate and for at least three times. Data are means ± SD. *, $p < .05$ versus control (BSA or phosphate-buffered saline). All the studies were done in triplicate. Abbreviations: BSA, bovine serum albumin; Col I, collagen type I; FN, fibronectin; GFU, colony-forming-unit; LAM, laminin; MSC, mesenchymal stem cell; PBS, phosphate-buffered saline.

expressed at much higher levels compared with cells cultured without the hydroxyapatite (Fig. 1E). These results were confirmed by western blot (Fig. 1F, 1G). Maximum expressions were detected at two hours. LLP2A-Ale increased MSC osteoblast differentiation and maturation (Fig. 1H, 1I).

LLP2A-Ale Partially and MSC + LLP2A-Ale Fully Restored Bone Loss and Strength Induced by Estrogen Deficiency

We next investigated the therapeutic potential of LLP2A-Ale, with or without the combination of MSC transplantation, in the treatment of OVX-induced bone loss, a standard preclinical model for osteoporosis.

We used anti-GFP staining to monitor if the transplanted MSCs homed to bone. In mice that received MSC transplantation, we could only detect few transplanted MSCs within bone marrow. In contrast, the GFP$^+$-MSCs were found at bone surface as osteoblast-like cells (Fig. 2A, yellow arrows) or embedded within bone matrix as osteocyte-like cells (Fig. 2A, white arrows). We also observed weak GFP+ staining within trabecular bone, presumably from previous two MSC IV injections that was associated with increased mineral appositions between MSC transplantations (Fig. 2A, light green arrows). We measured bone turnover by serum bone markers (PINP, osteocalcin, and CTX-1) and surface-based bone histomorphometry. Fourteen weeks after the ovariectomy (12 weeks after treatment), PINP, osteocalcin, osteoblast surface, and bone formation rate/ BS were approximately 10%–20% higher in LLP2A-Ale or PTH treated groups as compared with PBS treated OVX mice (Fig. 3A; Supporting Information Fig. S1A). Although osteoblast surface were approximately 20% higher in MSC treated group compared with the OVX group, bone formation rate/BS (BFR/BS) was similar to OVX group. This was found to be from a reduced mineralizing surface in this MSC-treated group compared with the ovariectomy group (Fig. 2A, 2B). By contrast, MSC + LLP2A-Ale increased serum osteocalcin, osteoblast surface ($p < .05$ compared OVX, MSC, LLP2A-Ale, and PTH) and bone formation rate by one- to threefold ($p < .05$ compared with OVX and MSC) (Fig. 2A, 2B; Supporting Information Fig. S1A). Osteoclast surface was higher in the OVX group ($p < .05$ vs. Sham) but lower in both the LLP2A-Ale and the MSC + LLP2A-Ale combination treatment group ($p < .05$ vs. OVX) (Supporting Information Fig. S1A). There were layers of osteoblasts-like cells in the MSC + LLP2A-Ale treatment group that formed osteoid bridges and connected the adjacent trabeculae (blue arrows), a critical step in the reestablishment of trabecular connectivity (Fig. 2B). These osteoblasts were very active as evidenced by increased mineral apposition rate (MAR) (yellow arrows, Fig. 2B). Twelve weeks after the treatment, while the OVX mice treated with PBS experienced more than 35% decrease in their vertebral trabecular BV, the group receiving two injections of LLP2A-Ale showed only a 45% trabecular bone gain relative to the OVX group ($p < .05$), which was similar to PTH-treated group. While MSC transplantation failed to increase bone mass, MSCs + LLP2A-Ale increased trabecular BV by more than 50% as compared to the OVX + PBS group ($p < .05$) and completely restored vertebral trabecular bone loss induced by OVX (Fig. 3A, 3C). Similarly, MSCs + LLP2A-Ale had a beneficial effect on trabecular bone strength. At 12-weeks post treatment, the increase in vertebral compression stress was approximately 15% higher than the OVX group ($p < .05$) (Fig. 3A).

Fourteen weeks after the ovariectomy (12 weeks after treatment), the OVX mice treated with PBS, MSC, or PTH experienced approximately 30% decrease in their endocortical bone formation rate. In contrast, endocortical bone formation

was increased by 46% and 66%, respectively, in mice treated with LLP2A-Ale or MSC + LLP2A-Ale ($p < .05$ compared with OVX + PBS, MSC, or PTH) (Fig. 3D). Twelve weeks after the treatment of OVX mice with either of MSC, LLP2A-Ale or PTH, there was no significant change in cortical bone thickness compared with the OVX group. However, cortical bone ultimate strength was increased by 19% ($p < .05$), respectively, in the OVX+ MSC + LLP2A-Ale –treated groups as compared to the OVX group (Fig. 3D).

We measured a number of cytokines in the serum reported to be associated with bone remodeling which included INF-γ, IL-1β, IL-6, IL-10, IL-12, KC, TNF-α, and TGF-β1. Among these cytokines, only TGF-β, IL-10, and INF-γ were within detectable limits in the serum. However, we found no differences among the different treatment groups for TGF-β1 and IL-10. INF-γ was 60% lower than OVX, MSC, and PTH ($p < .05$ compared with sham) while LLP2A-Ale or MSC + LLP2A-Ale treatments prevented the decrease of INF-γ induced by OVX (Supporting Information Fig. S2).

LLP2A-Ale Increased and MSC + LLP2A-Ale Further Augmented Bone Formation in Adult and in Aged Mice

As aging might be associated with the reduced number of the MSCs in bone marrow and the supportive microenvironment required maintaining the MSC osteoblast differentiation [4,5], we evaluated the effects of LLP2A-Ale in the augmentation of bone formation in the skeleton of matured (24-week-old) or aged (24-month-old) female C57BL/6 mice.

In 24-week-old mice, the transplanted MSCs were observed at trabecular bone surface that some if not all of them were also osteocalcin positive (Fig. 2B, white arrows). When compared with the PBS-treated group, LLP2A-Ale increased osteoblast surface by 154%, MS/BS by 25% and BFR/BS by 79% ($p < .05$, Fig. 3A). MSC + LLP2A-Ale significantly increased osteocalcin by 87%, osteoblast surface by 180%, MS/BS by 80%, MAR by 62%, and BFR/BS by 191% (all $p < .05$ vs. PBS and MSC; Fig. 3A; Supporting Information Fig. S1B) compared with the PBS control group. PTH increased osteoblast surface by 103%, MAR by 38%, and BFR/BS by 59% from the PBS control (Fig. 4A; Supporting Information Fig. S1B). Serum CTX-1 and osteoclast surface did not change significantly among the groups (Supporting Information Fig. S1B). Trabecular BV in the fifth vertebral bodies were approximately 30% higher in MSC + LLP2A-Ale and PTH groups compared with the PBS or MSC groups ($p < .05$); however, vertebral strength (maximum stress) was higher only in MSC + LLP2A-Ale group ($p < .05$ vs. PBS) (Fig. 4A). Osteoblasts in the MSC + LLP2A-Ale group appeared larger than those without MSC transplantation groups (Fig. 4B) and had more double labeled surface and higher mineral apposition compared with PBS, MSC, or PTH control groups (Fig. 4B).

Increased endocortical and periosteal bone formation was accompanied by increased cortical bone thickness (8%) and a 32% increase in the ultimate strength in the MSC + LLP3A-Ale group compared with PBS ($p < .05$ vs. PBS) (Fig. 4C, 4D).

In the 24-month-old mice, the transplanted MSCs were observed within bone marrow in group that only received MSC transplantation. In contrast, the transplanted MSCs were observed at trabecular bone surface that coexpressed osteocalcin (Fig. 2C, white arrows) and within bone matrix as osteocytes in the MSC + LLP2A-Ale group. LLP2A-Ale increased osteocalcin by 113% osteoblast surface by 22%, MS/BS by 20% and BFR/BS by 35% (Fig. 5A; Supporting Information
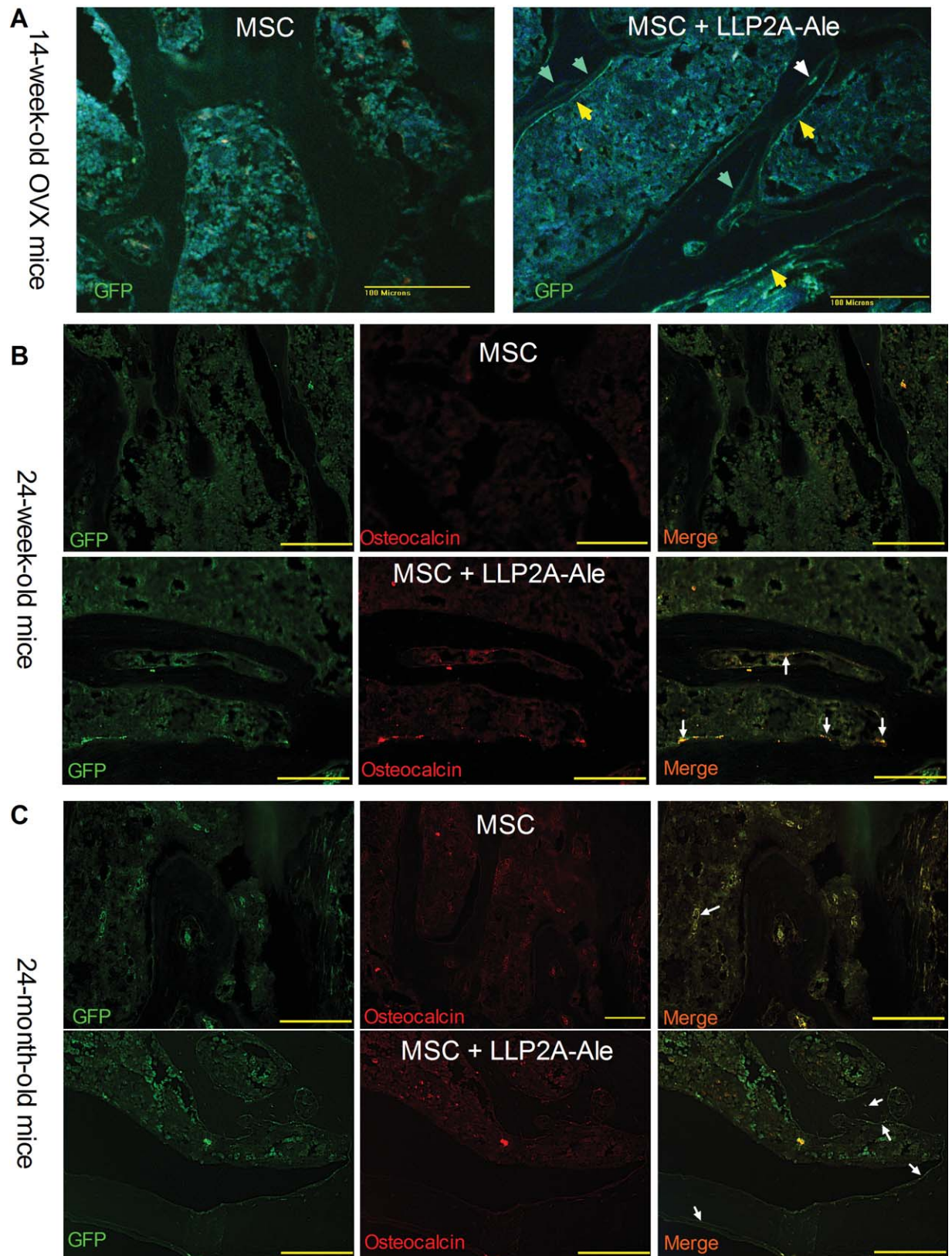
Figure 2. Mesenchymal stem cells (MSCs) bone homing and osteoblast differentiation following LLP2A-Ale treatment. **(A):** Representative decalcified vertebral body sections were obtained from ovariectomized mice that received three injections of MSC or MSC + LLP2A-Ale. The transplanted MSCs were accessed by anti-green fluorescent protein (GFP) staining (green) at week 14 of the study. **(B):** Representative decalcified vertebral body sections were obtained from 24-week-old mice that received two injections of MSC or MSC + LLP2A-Ale. The transplanted MSCs were stained in green, osteocalcin were stained in red. Cells that were positive for both GFP and osteocalcin appeared in yellow. **(C):** Representative decalcified vertebral body sections were obtained from 24-month-old mice that received two injections of MSC or MSC + LLP2A-Ale. The transplanted MSCs were stained in green, osteocalcin were stained in red. Cells that were positive for both GFP and osteocalcin appeared in yellow. Abbreviations: MSC, mesenchymal stem cell; GFP, green fluorescent protein.
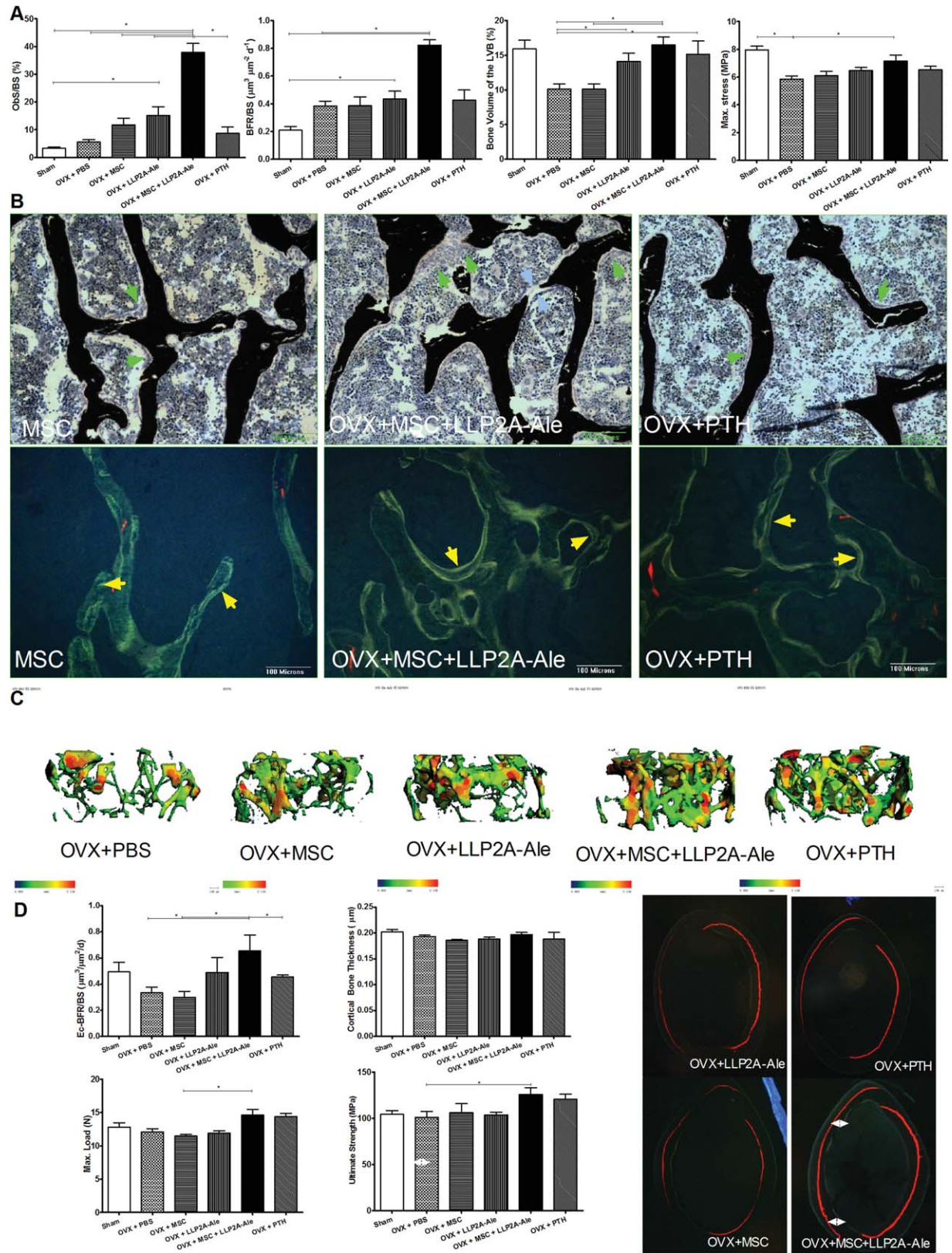
Figure 3. LLP2A-Ale or with the combination of mesenchymal stem cell (MSC) transplantation increased bone formation in OVX mice. Two-month-old C57BL/6 were ovariectomized (OVX) and left untreated for 4 weeks. They were then treated with phosphate-buffered saline (PBS), MSC (5×10^5), LLP2A-Ale (0.9 nmol/mouse, IV at weeks 2, 6, and 10), MSC + LLP2A-Ale (LLP2A-Ale, 0.9 nmol/mouse; MSC 5×10^5 per mouse, IV at weeks 2, 6, and 10), or human parathyroid hormone (PTH 1-34) (30 μg/kg, three times per week). Mice were killed at week 16. Alizarin red was injected before the treatments and two tetracycline injections were given 7 and 2 days before the mice were killed. **(A):** Osteoblast surface, bone formation rate, bone volume, and maximum stress were measured from the lumbar vertebral bodies. **(B):** Representative sections from the lumbar vertebral bodies that were stained in tetrachrome and von *kossa* or left unstained. Bone was stained in black. Green arrow heads illustrate osteoblasts at the bone surface. Blue arrow heads illustrates osteotoid bridge. Yellow arrows illustrate double tetracycline-labeled bone surfaced. **(C):** Representative trabecular thickness maps were obtained from the distal femurs by micro-CT where the trabecular thickness is color coded with blue-green color-codes thinner trabeculae while yellow-red color-codes thicker trabeculae. **(D):** Endocortical bone formation rate, cortical bone thickness, maximum load, and ultimate strength were measured at the right femurs. Double-side white arrows illustrate total bone gain at the endocortical compartments during the treatment period. *, $p < .05$ between the indicated groups. Abbreviations: Obs, osteoblast surface; BFR, bone formation rate; BS, bone surface; LVB, lumbar vertebral body; MSC, mesenchymal stem cell; OVX, ovariectomized; PBS, phosphate-buffered saline; PTH, parathyroid hormone.
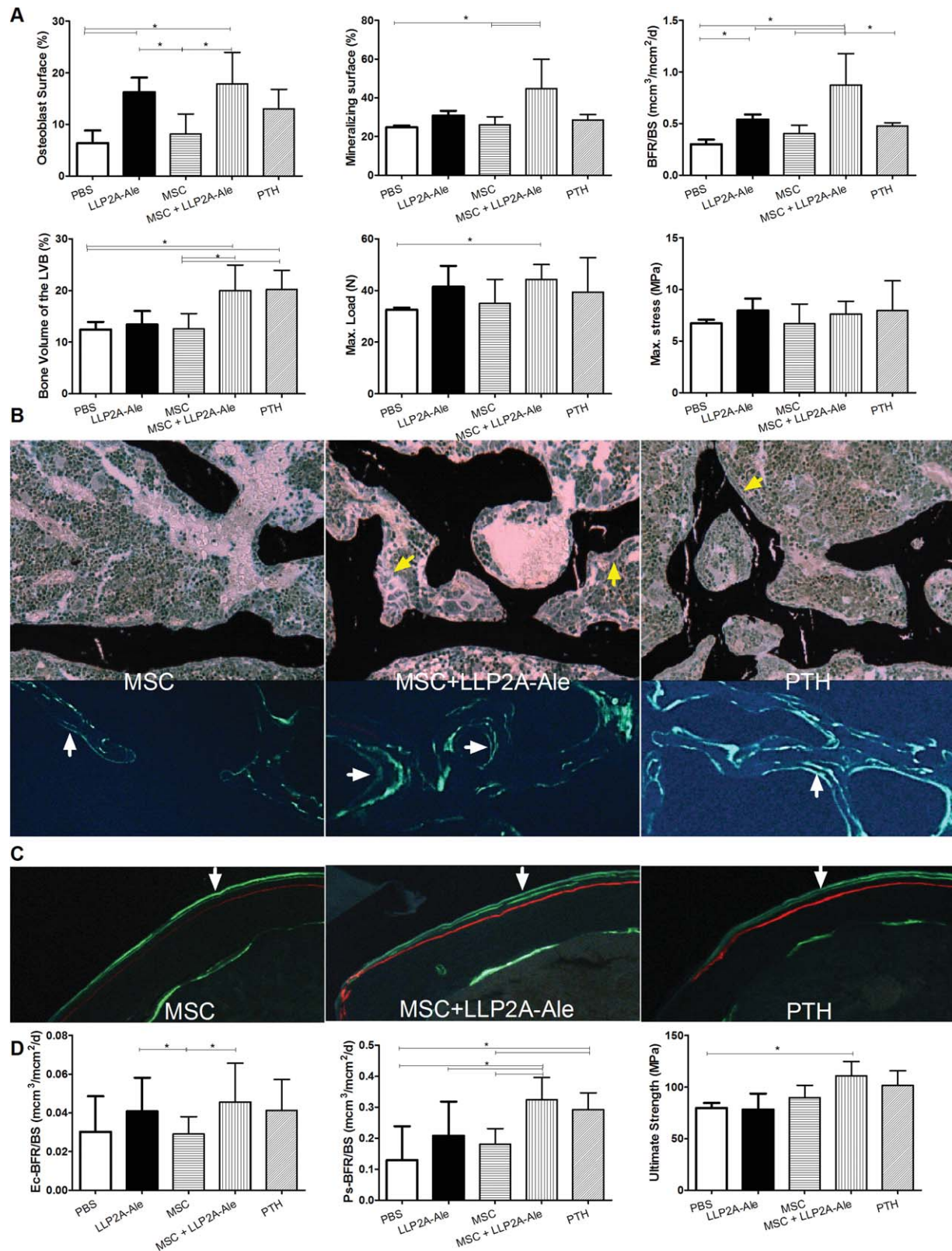
Figure 4. LLP2A-Ale or with the combination of mesenchymal stem cell (MSC) transplantation increased trabecular and cortical bone formation and strength in adult mice. Female mice of 24-week-old were treated with phosphate-buffered saline (PBS), MSC (1x 10^5), LLP2A-Ale (0.9 nmol/mouse, IV at baseline and week 6), MSC + LLP2A-Ale (LLP2A-Ale, 0.9 nmol/mouse; MSC 5 × 10^5 per mouse, IV at baseline and week 6), or human PTH (1-34) (30 μg/kg, five times per week). Mice were killed at week 12. Alizarin red was injected before the treatments and two calcein injections were given 9 and 2 days before the mice were killed. **(A):** Osteoblast surface, mineralizing surface, bone formation rate, bone volume, maximum load, and stress were measured from the lumbar vertebral bodies. **(B):** Representative sections that were stained in tetrachrome and von *kossa* or left unstained. Bone was stained in black. Green arrows illustrates osteoblasts at the bone surface, white arrows illustrate double calein-labeled bone surfaces. **(C):** Representative cortical bone sections and **(D):** bone formation rates measured at the endocortical and periosteal surfaces, ultimate strength of the femurs. White arrows illustrate double calein-labeled periosteal bone surface.*, $p < .05$ between the indicated groups. Abbreviations: BFR, bone formation rate; BS, bone surface; LVB, lumbar vertebral body; MSC, mesenchymal stem cell; PBS, phosphate-buffered saline; PTH, parathyroid hormone.
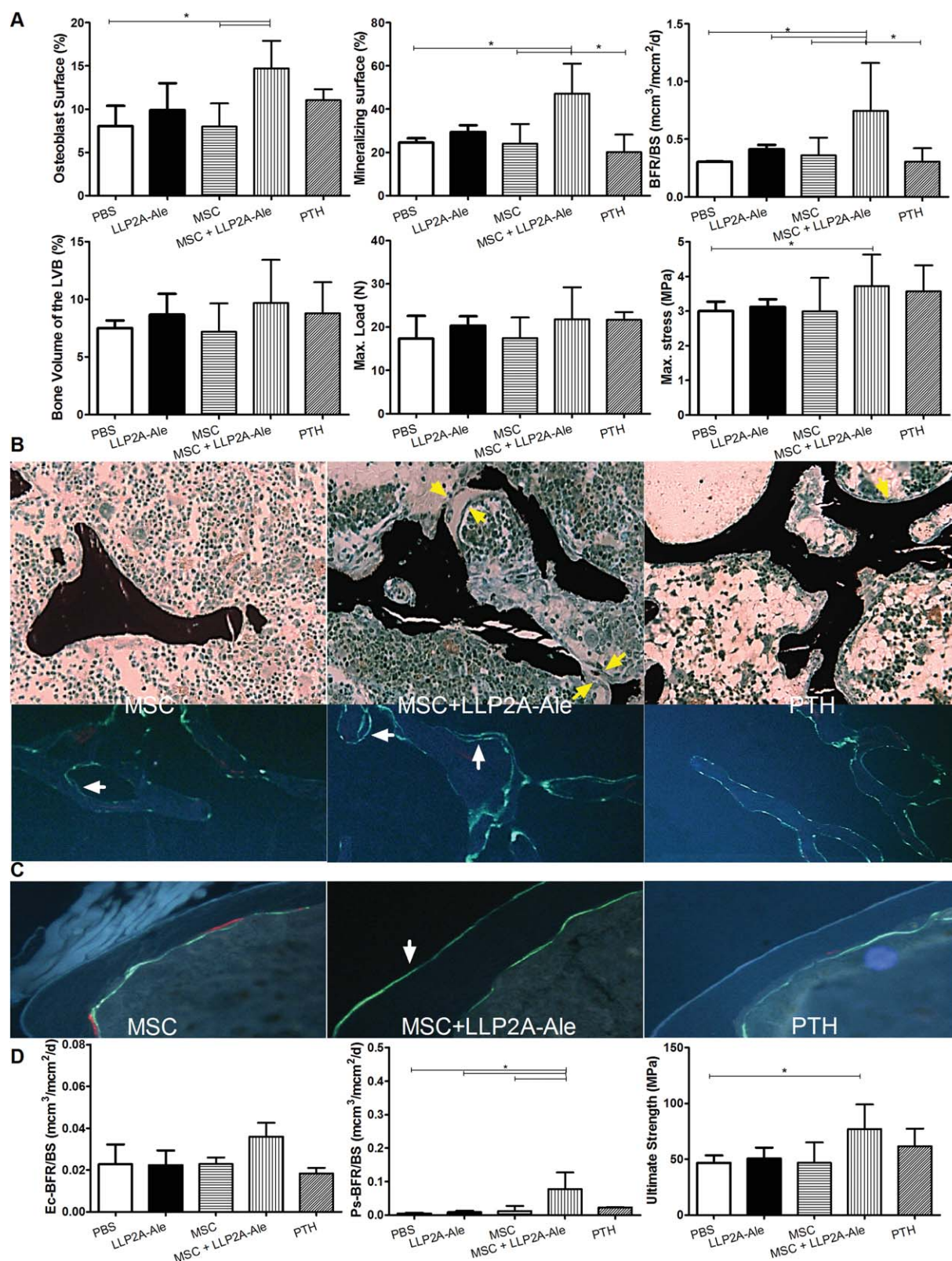
Figure 5. Combination treatment of mesenchymal stem cell (MSC) and LLP2A-Ale increased trabecular and cortical bone formation and bone volume (BV) in aged mice. Female mice of 24-month-old were treated with phosphate-buffered saline (PBS), MSC (5×10^5), LLP2A-Ale (0.9 nmol/mouse, IV at baseline and week 6), MSC + LLP2A-Ale (LLP2A-Ale, 0.9 nmol/mouse; MSC 5×10^5 per mouse, IV at baseline and week six), or human PTH (1-34) (30 μg/kg, five times per week). Mice were killed at week 12. Alizarin red was injected before the treatments and two calcein injections were given 9 and 2 days before the mice were killed. **(A):** Osteoblast surface, mineralizing surface, bone formation rate, BV, maximum load, and stress were measured from the lumbar vertebral bodies. **(B):** Representative sections that were stained in tetrachrome and von *kossa* or left unstained. Bone was stained in black. Green arrows illustrates osteoblasts and osteoid bridging the trabeculae in the MSC + LLP2A-Ale treated group; white arrows illustrate double calein-labeled bone surfaces. **(C):** Representative cortical bone sections and **(D):** bone formation rates measured at the endocortical and periosteal surfaces, ultimate strength of the femurs. White arrows illustrate calein-labeled periosteal bone surface.*, $p < .05$ between the indicated groups. Abbreviations: BFR, bone formation rate; BS, bone surface; LVB, lumbar vertebral body; PBS, phosphate-buffered saline; MSC, mesenchymal stem cell; PTH, parathyroid hormone.

Fig. S1C) when compared with the PBS-treated group. However, none of these increases reached a statistically significant level, as compared to PBS. Serum CTX-1 and osteoclast surface did not change significantly in any of the treatment groups (Fig. S1C). MSC + LLP2A-Ale significantly increased MS/BS by 72%, BFR/BS by 192%, serum osteocalcin by 278%, and vertebral maximum stress by 18% as compared to all the other groups ($p < .05$ for all of these parameters vs. PBS; Fig. 5A; Supporting Information Fig. S1C). Osteoblast bridges were frequently present in the trabecular bone of the mice treated with LLP2A-Ale and MSC + LLP2A-Ale (Fig. 5B). No significant changes in bone formation parameters were found in PTH in relative to the PBS-treated group (Fig. 5).

Cortical bone thickness increased by 6% in MSC + LLP2A-Ale and by 6% in PTH-treated group as compared to the PBS-treated group. MSC + LLP2A-Ale increased periosteal bone formation rate by more than 2000% and cortical bone ultimate strength by 30% as compared to the PBS-treated group ($p < .05$; Fig. 5C, 5D).

DISCUSSION

We have developed a synthetic high affinity $\alpha4\beta1$ integrin ligand (LLP2A), which, when conjugated to alendronate, becomes a bone seeking agent (U.S. Provisional Patent Application No. 61/379,643). This report is an expansion of a previous "proof-of-concept" study on the technology, in which we used a single IV MSC injection with or without LLP2A-Ale in an xenotransplantation model and in the prevention of rapid bone loss induced by estrogen deficiency [20]. Our current studies extended these observations in animal models of clinically relevant bone diseases including estrogen deficiency and aging to demonstrate the efficacy of bone homing of MSCs with LLP2A-Ale to treat established bone loss. We found that this hybrid compound, LLP2A-alendronate (LLP2A-Ale), increased the phosphorylation of the Akt kinase and that was associated with increased MSC migration and osteogenesis. LLP2A-Ale increased the numbers of transplanted MSCs adjacent to the bone surface, embedded within the bone matrix and increased bone mass and bone strength in estrogen deficiency and aging models of osteoporosis in mice.

Extracellular matrix (ECM) made by bone marrow cells, including FN, LAM and collagens, play important roles in the maintenance of MSC function, migration, and osteoblast differentiation [27]. The adhesion of the integrins to the ECM disarms cell adhesion and drives cell migration. For example, $\alpha5\beta1$-integrin-mediated adhesion of osteoblasts is more effective than $\alpha v\beta3$-mediated adhesions on FN and results in more cell migration [35]. Additionally, the stiffness of the ECM also affects cell fate [36,37]. At the same time, stem cells can also exert a mechanical force on collagen fibers and give feedback to alter cell-fate decisions [38]. MSCs are more likely to differentiate into osteoblastic lineage when the stiffness of the matrix in which they are embedded is more rigid and contains hydroxyapatite [39,40]. This study demonstrated that both LLP2A and LLP2A-Ale induced MSC migration was differentially affected by cell adhesion to specific ECM ligands. In particular, Col I-rich matrix was a crucial regulator of LLP2A-mediated mesenchymal cell migration. Furthermore, Col I, but not LAM or FN, was associated with accelerated MSC migration in responding to LLP2A-Ale treatment especially when the hydroxyapatite was present. Thus, Col I

may accelerate MSCs migration toward hydroxyapatite/bone following LLP2A-Ale treatment.

Phosphorylation of receptor tyrosine kinases (RTKs) RTKs is required for the stem cell migratory response [33,41]. We studied Akt, a serine threonine kinase that provides a powerful survival signal for cells and may prevent the transplanted MSC from undergoing apoptosis [42], and reported activation of Akt in murine MSCs in response to LLP2A-Ale stimulation. Inhibition of Akt is reported to led to reduced MSC osteogenic potential [43], while Akt promotes BMP2-mediated osteoblast differentiation [44]. Genetically modified MSCs that overexpress Akt facilitated the repair of infarcted heart tissue by increasing the homing and retention of the transplanted MSCs in the damaged heart [42]. Akt phosphorylation is also the main mechanism associated with PTH's protective effects on osteoblast and osteocyte viability in a glucocorticoid excess model [45]. These data support our previous finding that treatment with LLP2A-Ale stimulated differentiation of the progenitor cells into osteoblasts [20]. Also, LLP2A-Ale activated other RTKs, especially when hydroxyapatite was present. One of these activated RTKs was the ribosomal protein 6. Ribosomal protein 6 was reported to regulate cell size and lifespan [46,47]. Together, mechanical adhesion to bone matrix protein (Col I) and mineral (hydroxyapatite) induces the activation of RTKs that are associated with accelerated MSC migration and osteoblast maturation following LLP2A-Ale treatment.

We found that 2–3 IV injections of LLP2A-Ale yielded comparable bone anabolic effects as those of daily PTH injection in mice. In the estrogen deficient bone loss model in mice, LLP2A-Ale increased serum osteocalcin, osteoblast surface, and bone formation rate and trabecular BV over the OVX group in both the lumbar vertebral body and the distal femurs. In adult female mice, LLP2A-Ale increased vertebral osteoblast surface, mineral apposition rate and bone formation rate. Bone resorption was increased by OVX and was lowered by LLP2A-Ale treatment to the sham-operated level and was not altered by LLP2A-Ale treatment in the intact animals. As the total alendronate dose in our compound from two IV injections was approximately [1/2]–1/5th of the therapeutic dose of alendronate over a 3-month treatment period, we did not observe any antiresorptive effects when bone turnover was relatively "normal" in the intact animals. However, LLP2A-Ale reduced bone resorption in the estrogen deficient state. Similar uncoupling of bone remodeling with bone formation exceeding bone resorption is also observed with other anabolic agents, including hPTH (1-34) [48] and sclerostin antibody [2,49]. The long-term effects of LLP2A-Ale on bone resorption certainly warrant further studies.

We have previously reported that one IV injection of LLP2A-Ale increased the bone homing, retention of the transplanted MSCs at the bone surface, and increased the osteoblast differentiation of the transplanted MSCs using an xenotransplantation model [20]. Our current studies confirm the ability of LLP2A-Ale in directing the transplanted MSCs to bone and enhanced their osteoblast differentiation in an established osteopenic skeleton following 14 weeks of estrogen deficiency. Moreover, our functional outcomes of osteogenesis in vivo using multiple outcome measures that include bone mass, turnover and strength measurements in two trabecular bone sites (distal femur and lumbar vertebral body) and cortical bone (mid-femur), Remarkably, three i.v. administrations of LLP2A-Ale plus MSCs further increased these bone formation parameters in trabecular bone. Additionally, the combination treatment induced higher rates of bone formation at both the endocortical and periosteal bone surfaces and resulted in higher cortical bone strength in the OVX animals.

In aged mice, while both LLP2A-Ale and PTH monotherapy failed to generate anabolic response, the combination treatment significantly increased bone formation parameters and translated into substantial increases in bone strength for both the trabecular and cortical bone sites. Additionally, there were increases in both osteoblasts and mineralizing surface suggesting either increased recruitment of the osteoblasts to bone surface or improved lifespan of the existing osteoblasts. The higher mineral apposition rates observed with LLP2A-Ale or the combination treatment suggest that osteoblast activity were increased and that there was more mineral being deposited and mineralized. Our finding from the adult mice (24-week-old) demonstrated that combination treatment of LLP2A-Ale and MSC was not superior to LLP2A-Ale monotherapy in these relatively young individuals. However, the addition of MSC transplantation to LLP2A-Ale may augment LLP2A-Ale efficacy and may allow for a complete restoration of bone trabecular and cortical BV and strength with profound bone loss either induced by prolong estrogen deficiency or advanced aging.

The MSCs may also have immunomodulatory effects that may alter the local bone marrow environment and augment bone formation. The MSCs are reported to exert a strong immunosuppressive effect on cells of both innate and adaptive immunity, such as on NK cells dendritic cells, T-cells and B cells [50–52]. One or two IV infusions of MSCs were shown to improve the survival rate in graft-versus-host disease model (GvHD) in mice and in humans [53–55]. The immunomodulatory effects of MSCs were associated with the secretion of cytokines and chemokines such as TGF-β, prostaglandin E_2, hepatocyte growth factor, IL-10, and interferon-gamma (IFN-γ) [52,53,56–59]. Among these cytokines, TGF-β1 is reported to be the most critical growth factor in coupling bone resorption with the endogenous stem cell recruitment to bone, and high-dose alendronate may blunt this action following PTH treatment [60,61]. As estrogen deficiency is associated with inflammatory responses that promote osteoclastogenesis [62], we monitored systemic cytokine levels following ovariectomy and MSC transplantation. Interestingly, we did not observe a change in levels of total serum TGF-β1 levels for any of the intervention studies. However we observed lower serum or gene expression. IFN-γ levels 14-weeks post-ovariectomy; this decrease was prevented in the LLP2A-Ale treated animals. As MSC transplantation by itself did not alter IFN-γ levels, the change in IFN-γ that we observed might be from LLP2A-Ale treatment rather than a direct therapeutic effect of MSCs on IFN-γ similar to what has been reported for the prevention of GvHD [63]. Nevertheless, prevention of the decline in IFN-γ levels by LLP2A-Ale may contribute to the antiproliferative, immunoregulatory and anti-inflammatory activities and is thus may be important in host defense mechanisms.

SUMMARY

In summary, LLP2A-Ale activated the Akt pathway and was associated with increased MSC migration, osteogenic differentiation of mesenchymal precursor cells especially in hydroxyapatite-rich environment. Our studies further established LLP2A-Ale as a vehicle to guide the transplanted MSCs to bone to treat bone loss related to aging and hormone deficiency. Additional preclinical and possibility clinical studies that further our understanding of the efficacy and toxicity LLP2A- Ale with and without MSC transplantation are now warranted.

DISCLOSURE OF POTENTIAL CONFLICTS OF INTEREST

The authors indicate no potential conflicts of interest.

REFERENCES

1   Black DM, Bilezikian JP, Ensrud KE et al. One year of alendronate after one year of parathyroid hormone (1–84) for osteoporosis. N Engl J Med 2005;353:555–565.

2   Li X, Ominsky MS, Warmington KS et al. Sclerostin antibody treatment increases bone formation, bone mass, and bone strength in a rat model of postmenopausal osteoporosis. J Bone Miner Res 2009;24:578–588.

3   Pittenger MF, Mackay AM, Beck SC et al. Multilineage potential of adult human mesenchymal stem cells. Science 1999;284:143–147.

4   Sethe S, Scutt A, Stolzing A. Aging of mesenchymal stem cells. Ageing Res Rev 2006;5:91–116.

5   Brack AS, Rando TA. Intrinsic changes and extrinsic influences of myogenic stem cell function during aging. Stem Cell Rev 2007;3:226–237.

6   Muschler GF, Nitto H, Boehm CA et al. Age- and gender-related changes in the cellularity of human bone marrow and the prevalence of osteoblastic progenitors. J Orthop Res 2001;19:117–125.

7   Zhang Y, Luo H, Zhang Z et al. A nerve graft constructed with xenogeneic acellular nerve matrix and autologous adipose-derived mesenchymal stem cells. Biomaterials 2010;31:5312–5324.

8   Schuleri KH, Feigenbaum GS, Centola M et al. Autologous mesenchymal stem cells produce reverse remodelling in chronic ischaemic cardiomyopathy. Eur Heart J 2009;30:2722–2732.

9   Pedram MS, Dehghan MM, Soleimani M et al. Transplantation of a combination of autologous neural differentiated and undifferentiated mesenchymal stem cells into injured spinal cord of rats. Spinal Cord 2010;48:457–463.

10 Hare JM, Fishman JE, Gerstenblith G et al. Comparison of allogeneic vs autologous bone marrow-derived mesenchymal stem cells delivered by transendocardial injection in patients with ischemic cardiomyopathy: The POSEIDON Randomized Trial. JAMA 2012;308:2369–2379.

11 Gutwald R, Haberstroh J, Kuschnierz J et al. Mesenchymal stem cells and inorganic bovine bone mineral in sinus augmentation: Comparison with augmentation by autologous bone in adult sheep. Br J Oral Maxillofac Surg 2010;48:285–290.

12 Vertenten G, Lippens E, Girones J et al. Evaluation of an injectable, photopolymerizable, and three-dimensional scaffold based on methacrylate-endcapped poly(D,L-lactide-co-epsilon-caprolactone) combined with autologous mesenchymal stem cells in a goat tibial unicortical defect model. Tissue Eng Part A 2009;15:1501–1511.

13 Longobardi L, Granero-Molto F, O'Rear L et al. Subcellular localization of IRS-1 in IGF-I-mediated chondrogenic proliferation, differentiation and hypertrophy of bone marrow mesenchymal stem cells. Growth Factors 2009;27:309–320.

14 Chapel A, Bertho JM, Bensidhoum M et al. Mesenchymal stem cells home to injured tissues when co-infused with hematopoietic cells to treat a radiation-induced multi-organ failure syndrome. J Gene Med 2003;5:1028–1038.

15 Granero-Molto F, Weis JA, Miga MI et al. Regenerative effects of transplanted mesenchymal stem cells in fracture healing. Stem Cells 2009;27:1887–1898.

16 Gao J, Dennis JE, Muzic RF et al. The dynamic in vivo distribution of bone marrow-derived mesenchymal stem cells after infusion. Cells Tissues Organs 2001;169:12–20.

17 Meyerrose TE, De Ugarte DA, Hofling AA et al. In vivo distribution of human adipose-derived mesenchymal stem cells in novel xenotransplantation models. Stem Cells 2007;25:220–227.

18 Cho SW, Sun HJ, Yang JY et al. Transplantation of mesenchymal stem cells overexpressing RANK-Fc or CXCR4 prevents bone loss in ovariectomized mice. Mol Ther 2009;17:1979–1987.

19 Peng L, Liu R, Marik J et al. Combinatorial chemistry identifies high-affinity peptidomimetics against alpha4beta1 integrin for in vivo tumor imaging. Nat Chem Biol 2006;2:381–389.

20 Guan M, Yao W, Liu R et al. Directing mesenchymal stem cells to bone to augment bone formation and increase bone mass. Nat Med 2012;18:456–462.

21 Herberg S, Hill WD. Two birds with one bone? IBMS BoneKEy 2012;9:1.

22 Yao W, Dai W, Shahnazari M et al. Inhibition of the progesterone nuclear receptor during the bone linear growth phase increases peak bone mass in female mice. Plos One 2010;5:e11410.

23 Yao W, Cheng Z, Shahnazari M et al. Overexpression of secreted frizzled-related protein 1 inhibits bone formation and attenuates parathyroid hormone bone anabolic effects. J Bone Miner Res 2010;25: 190–199.

24 Yao W, Cheng Z, Pham A et al. Glucocorticoid-induced bone loss in mice can be reversed by the actions of parathyroid hormone and risedronate on different pathways for bone formation and mineralization. Arthritis Rheum 2008;58:3485–3497.

25 Dempster DW, Compston JE, Drezner MK et al. Standardized nomenclature, symbols, and units for bone histomorphometry: A 2012 update of the report of the ASBMR Histomorphometry Nomenclature Committee. J Bone Miner Res 2013;28:2–17.

26 Turner CH, Burr DB. Basic biomechanical measurements of bone: A tutorial. Bone 1993;14:595–608.

27 Chen XD, Dusevich V, Feng JQ et al. Extracellular matrix made by bone marrow cells facilitates expansion of marrow-derived mesenchymal progenitor cells and prevents their differentiation into osteoblasts. J Bone Miner Res 2007;22:1943–1956.

28 Zhu H, Mitsuhashi N, Klein A et al. The role of the hyaluronan receptor CD44 in mesenchymal stem cell migration in the extracellular matrix. Stem Cells 2006;24:928–935.

29 Lin H, Yang G, Tan J et al. Influence of decellularized matrix derived from human mesenchymal stem cells on their proliferation, migration and multi-lineage differentiation potential. Biomaterials 2012;33:4480–4489.

30 Lee SH, Lee YJ, Han HJ. Role of hypoxia-induced fibronectin-integrin beta1 expression in embryonic stem cell proliferation and migration: Involvement of PI3K/Akt and FAK. J Cell Physiol 2011;226:484–493.

31 Lee DH, Park BJ, Lee MS et al. Chemotactic migration of human mesenchymal stem cells and MC3T3-E1 osteoblast-like cells induced by COS-7 cell line expressing rhBMP-7. Tissue Eng 2006;12:1577–1586.

32 Zhang Q, Liu G, Wu Y et al. BDNF promotes EGF-induced proliferation and migration of human fetal neural stem/progenitor cells via the PI3K/Akt pathway. Molecules 2011;16:10146–10156.

33 Veevers-Lowe J, Ball SG, Shuttleworth A et al. Mesenchymal stem cell migration is regulated by fibronectin through alpha5beta1-integrin-mediated activation of PDGFR-beta and potentiation of growth factor signals. J Cell Sci 2011;124:1288–1300.

34 Ryu CH, Park SA, Kim SM et al. Migration of human umbilical cord blood mesenchymal stem cells mediated by stromal cell-derived factor-1/CXCR4 axis via Akt, ERK, and p38 signal transduction pathways. Biochem Biophys Res Commun 2010;398:105–110.

35 Huveneers S, Truong H, Fassler R et al. Binding of soluble fibronectin to integrin alpha5 beta1 - link to focal adhesion redistribution and contractile shape. J Cell Sci 2008;121:2452–2462.

36 Discher DE, Janmey P, Wang YL. Tissue cells feel and respond to the stiffness of their substrate. Science 2005;310:1139–1143.

37 Engler AJ, Sen S, Sweeney HL et al. Matrix elasticity directs stem cell lineage specification. Cell 2006;126:677–689.

38 Zeiger AS, Loe FC, Li R et al. Macromolecular crowding directs extracellular matrix organization and mesenchymal stem cell behavior. Plos One 2012;7:e37904.

39 Cieslik M, Mertas A, Morawska-Chochol A et al. The evaluation of the possibilities of using PLGA co-polymer and its composites with carbon fibers or hydroxyapatite in the bone tissue regeneration process – in vitro and in vivo examinations. Int J Mol Sci 2009;10:3224–3234.

40 Fu J, Wang YK, Yang MT et al. Mechanical regulation of cell function with geometrically modulated elastomeric substrates. Nat Methods 2010;7:733–736.

41 Ip JE, Wu Y, Huang J et al. Mesenchymal stem cells use integrin beta1 not CXC chemokine receptor 4 for myocardial migration and engraftment. Mol Biol Cell 2007;18:2873–2882.

42 Mangi AA, Noiseux N, Kong D et al. Mesenchymal stem cells modified with Akt prevent remodeling and restore performance of infarcted hearts. Nat Med 2003;9:1195–1201.

43 Fierro F, Illmer T, Jing D et al. Inhibition of platelet-derived growth factor receptorbeta by imatinib mesylate suppresses proliferation and alters differentiation of human mesenchymal stem cells in vitro. Cell Prolif 2007;40:355–366.

44 Mukherjee A, Rotwein P. Akt promotes BMP2-mediated osteoblast differentiation and bone development. J Cell Sci 2009;122:716–726.

45 Weinstein RS, Jilka RL, Almeida M et al. Intermittent parathyroid hormone administration counteracts the adverse effects of glucocorticoids on osteoblast and osteocyte viability, bone formation, and strength in mice. Endocrinology 2010;151:2641–2649.

46 Selman C, Tullet JM, Wieser D et al. Ribosomal protein S6 kinase 1 signaling regulates mammalian life span. Science 2009;326:140–144.

47 Ruvinsky I, Meyuhas O. Ribosomal protein S6 phosphorylation: From protein synthesis to cell size. Trends Biochem Sci 2006;31:342–348.

48 Sato M, Vahle J, Schmidt A et al. Abnormal bone architecture and biomechanical properties with near-lifetime treatment of rats with PTH. Endocrinology 2002;143:3230–3242.

49 Li X, Warmington KS, Niu QT et al. Inhibition of sclerostin by monoclonal antibody increases bone formation, bone mass, and bone strength in aged male rats. J Bone Miner Res 2010;25:2647–2656.

50 Nauta AJ, Fibbe WE. Immunomodulatory properties of mesenchymal stromal cells. Blood 2007;110:3499–3506.

51 Fibbe WE, Nauta AJ, Roelofs H. Modulation of immune responses by mesenchymal stem cells. Ann N Y Acad Sci 2007;1106:272–278.

52 Ren G, Zhang L, Zhao X et al. Mesenchymal stem cell-mediated immunosuppression occurs via concerted action of chemokines and nitric oxide. Cell Stem Cell 2008;2:141–150.

53 Yanez R, Lamana ML, Garcia-Castro J et al. Adipose tissue-derived mesenchymal stem cells have in vivo immunosuppressive properties applicable for the control of the graft-versus-host disease. Stem Cells 2006;24:2582–2591.

54 Ball LM, Bernardo ME, Roelofs H et al. Cotransplantation of ex vivo expanded mesenchymal stem cells accelerates lymphocyte recovery and may reduce the risk of graft failure in haploidentical hematopoietic stem-cell transplantation. Blood 2007;110:2764–2767.

55 Agholme F, Li X, Isaksson H et al. Sclerostin antibody treatment enhances metaphyseal bone healing in rats. J Bone Miner Res 2010; 25:2412–2418.

56 Ponte AL, Marais E, Gallay N et al. The in vitro migration capacity of human bone marrow mesenchymal stem cells: Comparison of chemokine and growth factor chemotactic activities. Stem Cells 2007;25: 1737–1745.

57 Byeon YE, Ryu HH, Park SS et al. Paracrine effect of canine allogenic umbilical cord blood-derived mesenchymal stromal cells mixed with beta-tricalcium phosphate on bone regeneration in ectopic implantations. Cytotherapy 2010;12:626–636.

58 Dao MA, Pepper KA, Nolta JA. Long-term cytokine production from engineered primary human stromal cells influences human hematopoiesis in an in vivo xenograft model. Stem Cells 1997;15:443–454.

59 Horwitz EM, Prather WR. Cytokines as the major mechanism of mesenchymal stem cell clinical activity: Expanding the spectrum of cell therapy. Isr Med Assoc J 2009;11:209–211.

60 Wu X, Pang L, Lei W et al. Inhibition of Sca-1-positive skeletal stem cell recruitment by alendronate blunts the anabolic effects of parathyroid hormone on bone remodeling. Cell Stem Cell 2010;7:571–580.

61 Tang Y, Wu X, Lei W et al. TGF-β1–induced migration of bone mesenchymal stem cells couples bone resorption with formation. Nat Med 2009;15:757–765.

62 Weitzmann MN, Cenci S, Rifas L et al. Interleukin-7 stimulates osteoclast formation by up-regulating the T-cell production of soluble osteoclastogenic cytokines. Blood 2000;96:1873–1878.

63 Polchert D, Sobinsky J, Douglas G et al. IFN-gamma activation of mesenchymal stem cells for treatment and prevention of graft versus host disease. Eur J Immunol 2008;38:1745–1755.

See www.StemCells.com for supporting information available online.